JOC Article
pubs.acs.org/joc

The Reversible Consecutive Mechanism for the Reaction of Trinitroanisole with Methoxide Ion

Vernon D. Parker,*[,†] Zhao Li,[†,‡] Kishan L. Handoo,[†] Weifang Hao,[†] and Jin-Pei Cheng[‡]

[†]*Department of Chemistry and Biochemistry, Utah State University, Logan, Utah 84322, United States, and* [‡]*Department of Chemistry, The State Key Laboratory of Elemento-Organic Chemistry, Nankai University, Tianjin 300071, China*

vernon.parker@usu.edu

Received September 20, 2010

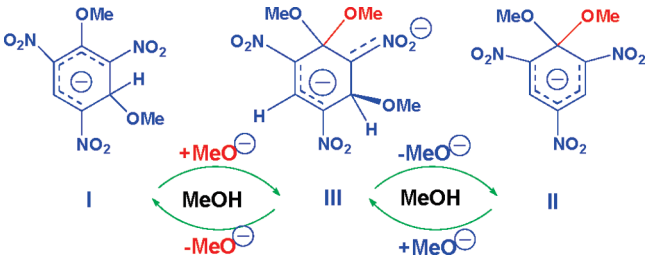

Although the competitive mechanism for Meisenheimer complex formation during the reaction of 2,4,6-trinitroanisole with methoxide ion in methanol is generally accepted, no kinetic evidence has been presented to rule out a reversible consecutive mechanism. Simulation of the competitive mechanism revealed that a fractional order in [MeO^-] is predicted by the latter. Conventional pseudo-first-order analysis of the kinetics resulted in cleanly first-order in [MeO^-], which rules out the competitive mechanism. The kinetic data are consistent with the reversible consecutive mechanism, which is proposed for this important reaction. An intermediate is required for this mechanism, and we propose that a dianion complex (**III**) is formed reversibly from the initial 1,3-σ complex (**I**). The trimethoxy complex (**III**), the ^{1}H NMR spectrum of which was observed earlier by Servis (Servis, K. L. *J. Am. Chem. Soc.* **1965**, *87*, 5495; **1967**, *89*, 1508), then eliminates methoxide ion reversibly to form the 1,1-σ complex product (**II**).

Introduction

The reactions of electron-deficient aromatic compounds with nucleophiles give rise to an important class of fundamental organic reactions, "nucleophilic aromatic substitution". Reactions of trinitroarenes exemplified by 1,3,5-trinitrobenzene (TNB) and 2,4,6-trinitroanisole (TNA), with both anionic and neutral nucleophiles, have been studied extensively.[1−25]

The reactions of TNA with alkoxide ions have received special attention in that both kinetically and thermodynamically

(1) Bunnett, J. F.; Morath, R. J. *J. Am. Chem. Soc.* **1955**, *77*, 5051.
(2) Ainscough, J. B.; Caldin, E. F. *J. Chem. Soc.* **1956**, 2528.
(3) Gold, V.; Rochester, C. H. *J. Chem. Soc.* **1964**, 1987.
(4) Bolles, T. F.; Drago, R. S. *J. Am. Chem. Soc.* **1965**, *87*, 5015.
(5) Crampton, M. R.; Gold, V. *J. Chem. Soc. B* **1966**, 893.
(6) (a) Servis, K. L. *J. Am. Chem. Soc.* **1965**, *87*, 5495. (b) Servis, K. L. *J. Am. Chem. Soc.* **1967**, *89*, 1508.
(7) Foster, R; Fyfe, C. A. *Tetrahedron* **1965**, *21*, 3363.
(8) Norris, A. R. *Can. J. Chem.* **1967**, *45*, 2703.
(9) Byrne, W. E.; Fendler, E. J.; Fendler, J. H.; Griffin, C. E. *J. Org. Chem.* **1967**, *32*, 2506.
(10) Buncel, E.; Norris, A. R.; Proudlock, W. *Can. J. Chem.* **1968**, *46*, 2759.
(11) Buncel, E.; Norris, A. R.; Russell, K. E. *Q. Rev., Chem. Soc.* **1968**, *22*, 123.
(12) Bernasconi, C. F. *J. Am. Chem. Soc.* **1968**, *90*, 4982.
(13) Fendler, E. J.; Griffin, C. E.; Fendler, J. H. *Tetrahedron Lett.* **1968**, 5631.
(14) Fendler, E. J.; Fendler, J. H.; Byrne, W.; Griffin, C. E. *J. Org. Chem.* **1968**, *33*, 4141.
(15) Buncel, E.; Norris, A. R.; Russell, K. E.; Proudlock, W. *Can. J. Chem.* **1969**, *47*, 4129.
(16) Fendler, J. H.; Fendler, E. J.; Griffin, C. E. *J. Org. Chem.* **1969**, *34*, 689.
(17) Crampton, M. R. *Adv. Phys. Org. Chem.* **1969**, *7*, 211.
(18) Fendler, E. J.; Fendler, J. H.; Griffin, C. E.; Larsen, J. W. *J. Org. Chem.* **1970**, *35*, 287.
(19) Bernasconi, C. F. *J. Am. Chem. Soc.* **1970**, *92*, 4682.
(20) Bernasconi, C. F. *J. Am. Chem. Soc.* **1971**, *93*, 6975.
(21) Bernasconi, C. F.; Bergstrom, R. G. *J. Org. Chem.* **1971**, *36*, 1325.
(22) Crampton, M. R.; Khan, H. A. *J. Chem. Soc., Perkin Trans. 2* **1972**, 733.
(23) Gan, L. H.; Norris, A. R. *Can. J. Chem.* **1974**, *52*, 8.
(24) Sasaki, M. *Rev. Phys. Chem. Jpn.* **1973**, *41*, 44.
(25) Fyfe, C. A.; Damji, S. W. H.; Koll, A. *J. Am. Chem. Soc.* **1979**, *101*, 956.

Published on Web 02/08/2011 DOI: 10.1021/jo101859n

SCHEME 1. Assumed Mechanism for the Formation of 1,3 (I)- and 1,1 (II)-Dimethoxy Complexes in Methanol Containing Methoxide Ion

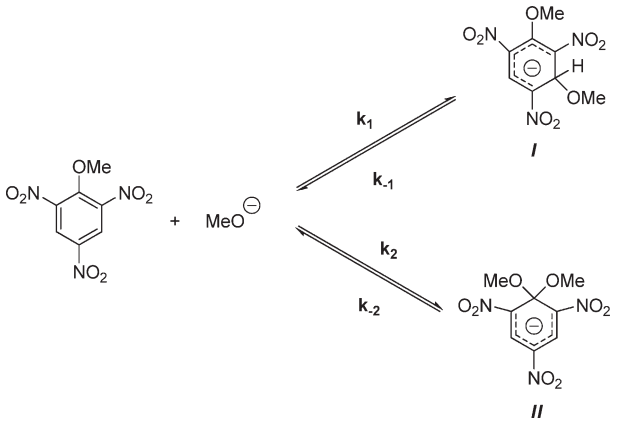

controlled Meisenheimer complexes have been observed. The work of Servis[6] in this respect has been of great importance in that he was able to follow the rapid formation of 2,4,6-trinitro-1,3-dimethoxy-cyclohexadienylide (**I**) and the slower formation of the 1,1-dimethoxy complex (**II**) by H^1 NMR spectroscopy. This work led to the assumption of the competitive mechanism illustrated in Scheme 1 and to thorough investigations of the energetics of these reactions by the Bernasconi[12,19−21] and the Fendler[13,14,16,18] groups. Bernasconi's and Fendler's kinetic and equilibrium data for the reactions of TNA with methoxide ion are summarized in Table 1.

TABLE 1. Rate and Equilibrium Constants for the Formation of 1,3-Dimethoxy and 1,1-Dimethoxy Complexes during the Reaction of TNA with Methoxide Ion in Methanol at 298 K, according to the Competitive Mechanism Shown in Scheme 1.[a]

$k_1/M^{-1}\,s^{-1}$	k_{-1}/s^{-1}	K_1/M^{-1}	$k_2/M^{-1}\,s^{-1}$	k_{-2}/s^{-1}	K_2/M^{-1}
950	350	2.71	17.3	0.00104	17 000

[a]References 14 and 20.

In contrast to the extensive work carried out on determining the apparent rate and equilibrium constants summarized in Table 1, no work to determine the mechanisms of the reactions was reported. It appears that the mechanisms shown in Scheme 1 were taken for granted by all workers in this area.

Results

The first question that must be addressed is whether or not complex **I** is on the reaction coordinate leading to complex **II**. If the latter is indeed the case, it is obvious that a single-step conversion of **I** to **II** is unlikely. This may account for the fact that the details of the mechanism have not been reported. However, it should be pointed out that determining whether the overall mechanism consists of two competing pathways (Scheme 1) or is a reversible consecutive mechanism in which complex **I** lies on the reaction coordinate for the formation of **II** is straightforward. The latter is the first task taken on in our reinvestigation of the mechanism of Meisenheimer complex formation during the reaction of TNA with methoxide ion in methanol.

Simulation of the Kinetics of the Competing Mechanism (Scheme 1). The kinetic data in Table 1 show that the reversible formation of complex **I** is rapid in comparison to the formation of complex **II** for the reaction of TNA with methoxide ion in methanol at 298 K. This fact allows the assumption that complex **I** is in equilibrium with reactants under the reaction conditions to be tested. Taking the latter into consideration leads to eq 1, which gives the equilibrium concentration of TNA as a function of

$$[\mathrm{TNA}]_{\mathrm{equil}} = [\mathrm{TNA}]_0/(K_1[\mathrm{MeO}^-]+1) \quad (1)$$

$$\mathrm{d}[\mathbf{II}]/\mathrm{d}t = k_2[\mathrm{MeO}^-][\mathrm{TNA}]_{\mathrm{equil}} = k_2[\mathrm{MeO}^-][\mathrm{TNA}]_0/(K_1[\mathrm{MeO}^-]+1) \quad (2)$$

its initial concentration, the equilibrium constant (K_1), and the methoxide ion concentration. Substitution of eq 1 into the rate law for formation of **II** gives eq 2, which describes the rate of the essentially irreversible formation of **II** before the latter becomes significant. Equation 2 suggests a fractional reaction order in [MeO^-] and that carrying out the kinetic study over a range of methoxide ion concentrations is the best way to probe for the applicability of Scheme 1.

Simulations were carried out by simple finite difference integration with the time for four half-lives divided into equal time increments, and $[TNA]_0$ was set equal to 0.0001 M. In the simulation, eq 2 was used for the first time step but required modification to eq 3 in subsequent steps. In each subsequent time step, $[TNA]_{start}$ was first evaluated by subtracting the accumulated concentration of **II** formed in previous steps from $[TNA]_0$. Numerical integration methods, in contrast to integrated rate

$$\mathrm{d}[\mathbf{II}]/\mathrm{d}t = k_2[\mathrm{MeO}^-][\mathrm{TNA}]_{\mathrm{start}}/(K_1[\mathrm{MeO}^-]+1) \quad (3)$$

equations, are associated with finite errors due to the sequential calculation of quantities. This error is minimized by using very small time steps. It is important to note that the derivations of eqs 1− 3 involve two assumptions: (a) complex **I** was assumed to be in equilibrium with reactants at all times during the reaction, and (b) the changes in [MeO^-] during reaction are negligible.

An effective way to test a finite difference simulation is to vary the length of the time steps. The values of parameters calculated are expected to change toward the true value as the length of the time steps is decreased. The simulations of the mechanism in Scheme 1 as a function of time step length are summarized in Table 2. The apparent second-order rate constants are labeled k_2' to differentiate them from the microscopic rate constant (k_2) specifically for the formation of complex II. The concentration of [MeO^-] in the simulations was varied from 15.0 to 120.0 mM, an 8-fold range. K_1 was taken to be equal to 2.71 M^{-1}, and k_2 was assumed to equal 17.3 $M^{-1}\,s^{-1}$. The ratios of the initial MeO^- to TNA concentrations ($[MeO^-]_0/[TNA]_0$) equal to 1200, 600, and 150, respectively, for simulations at $[MeO^-]_0$ equal to 120, 60, and 15 mM, satisfy the pseudo-first-order condition.

The apparent pseudo-first-order rate constants (k_{app}) in Table 2 vary considerably from the expected 2-fold change for a 2-fold decrease in [MeO^-], verifying the fractional reaction order. These results provide an excellent guide for the experimental investigation. The data in Table 3 verify the time independence of k_{app} as well. The slight variations in the rate constants as the length of the time steps are decreased

TABLE 2. Simulation of the Kinetics of the Reaction of TNA with Methoxide Ion in Methanol according to Scheme 1 Applying Input Data from Table 1

	[MeO$^-$] = 120 mM simulation time = 2 s		[MeO$^-$] = 60 mM simulation time = 4 s		[MeO$^-$] = 15 mM simulation time = 16 s	
no. points	k_{app}/s^{-1a}	k_2'/M^{-1} s^{-1b}	k_{app}/s^{-1a}	k_2'/M^{-1} s^{-1b}	k_{app}/s^{-1a}	k_2'/M^{-1} s^{-1b}
1000	1.5690	13.075	0.8944	14.907	0.2499	16.660
2000	1.5677	13.064	0.8936	14.893	0.2496	16.640
4000	1.5672	13.060	0.8932	14.887	0.2495	16.633
7000	1.5669	13.058	0.8930	14.883	0.2494	16.627
10 000	1.5667	13.056	0.8929	14.882	0.2494	16.627

[a]Apparent pseudo-first-order rate constant. [b]Apparent second-order rate constant.

TABLE 3. Test for Linearity of ln(1 − ER) from the 10 000 Point Simulation with [MeO$^-$] Equal to 120 mM

points in correlation	k_{app}/s^{-1}	k_2'/M^{-1} s^{-1}
1−10	1.5668	13.057
1−100	1.5668	13.057
1−1000	1.5668	13.057
1−2000	1.5668	13.057
1−10000	1.5667	13.056

show that none of rate constants are in serious error and those obtained in the 10 000 point simulations are most reliable.

The linearity test provided by the data in Table 3 shows that simulated kinetic data for the competitive mechanism described in Scheme 1, under the conditions given, show no deviations from first-order behavior over the first four half-lives of the reaction.

Experimental Investigation of the Applicability of Scheme 1 to the Reactions of TNA with Methoxide Ion in Methanol at 293 K. Contrary to the expectation according to Scheme 1, the second-order rate constants (k_2') in Table 4 were observed to be independent of [MeO$^-$]. The values of k_2' vary from 11.48 to 11.83 M^{-1} s^{-1} with an average percent deviation of ±0.7%. Furthermore, the variations show no relationship to [MeO$^-$]. We attribute these variations to experimental error. The latter should be compared to the [MeO$^-$]-dependent variations in the simulated data in Table 2. The simulated value of k_2 was observed to be equal to 13.06 M^{-1} s^{-1} ([MeO$^-$]$_0$ = 120 mM) and 16.63 M^{-1} s^{-1} ([MeO$^-$]$_0$ = 15 mM).

TABLE 4. Experimental Rate Constants for the Reaction of TNA (0.0001 M) with Methoxide Ion in Methanol at 293 K

[MeO$^-$]/mM	number $t_{0.5}$	k_{app}/s^{-1a}	k_2'/M^{-1} s^{-1b}
120	4	1.405	11.71
60	4	0.689	11.48
15	4	0.1772	11.81
120	3	1.403	11.69
60	3	0.698	11.63
15	3	0.1751	11.67
120	2	1.397	11.64
60	2	0.694	11.57
15	2	0.1738	11.59
120	1	1.383	11.53
60	1	0.689	11.48
30	1	0.355	11.83
15	1	0.1738	11.59
		av ± av % dev	11.63 ± 0.7%

[a]Experimental pseudo-first-order rate constant. [b]Apparent second-order rate constant.

The data in Table 4 are supported by the first-order plots as a function of reaction period illustrated in Figures 1−3 for cases where [MeO$^-$] was 15 mM (Figure 1), 60 mM (Figure 2), and 120 mM (Figure 3). Raw data were used in the linear correlations without any further treatment. For the 4 $t_{0.5}$ data, there is scatter in the data at long times but no indication of nonlinearity.

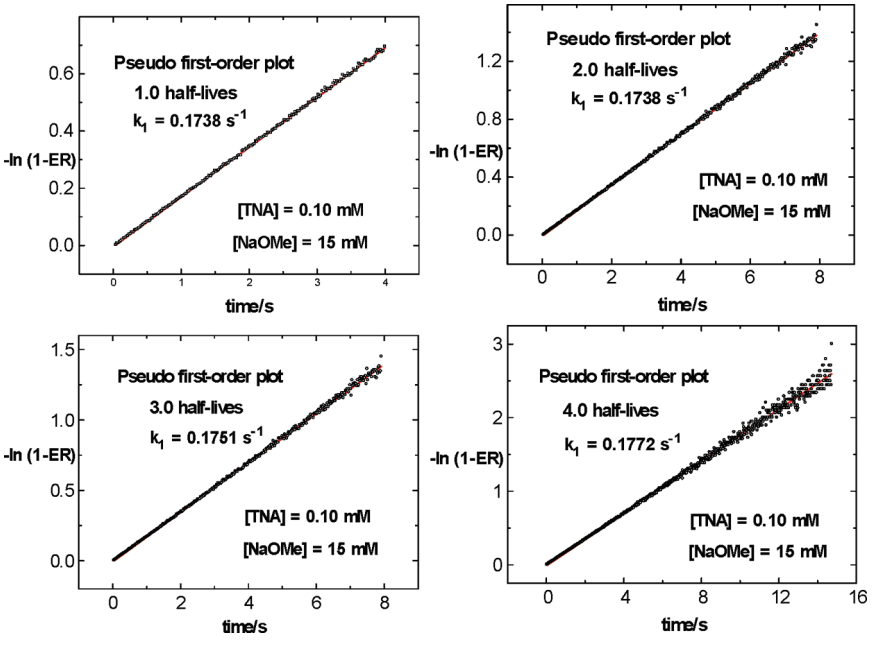

FIGURE 1. Pseudo-first-order plots for the reaction of TNA with [MeO$^-$] equal to 15 mM.

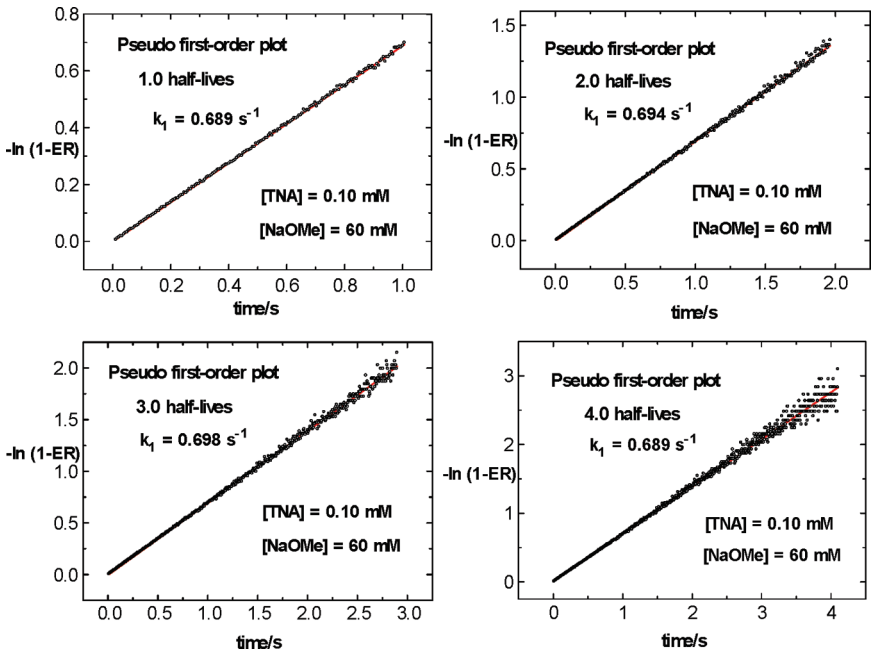

FIGURE 2. Pseudo-first-order plots for the reaction of TNA with [MeO^-] equal to 60 mM.

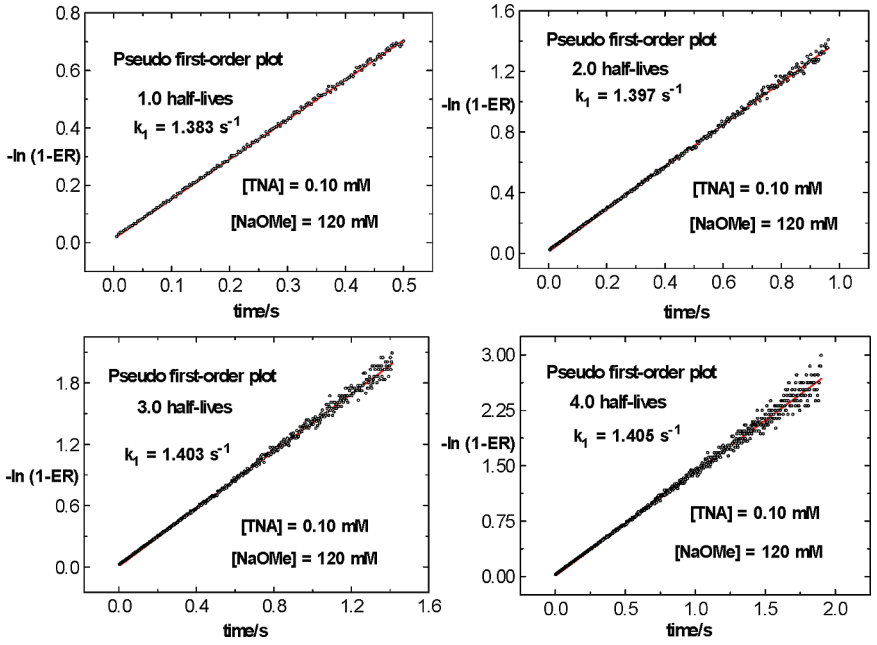

FIGURE 3. Pseudo-first-order plots for the reaction of TNA with [MeO^-] equal to 120 mM.

The data in Table 4 and Figures 1−3 are clearly inconsistent with the competitive reaction mechanism in Scheme 1, which requires the second-order rate constants to increase with decreasing values of $[MeO^-]_0$, and suggest that complex **I** is an intermediate during the formation of complex **II**.

The data in Table 5 were obtained using a modification of the pseudo-first-order analysis procedure. The experimental procedure involved recording 2000 point absorbance−time (abs−*t*) profiles over about the first half-lives of the reactions and doing a sequential first-order analysis on specific point segments of the abs−*t* profiles. The procedure also employed least-squares linear correlation, but in this case, 24 different analyses were carried out over different point segments in the profile. The point segments include points 1−11, 1−21, 1−31, 1−41, 1−51, 1−101, 1−201, 1−301, 1−401, 1−501, 1−601, 1−701, 1−801, 1−901, 1−1001, 1−1101, 1−1201, 1−1301, 1−1401, 1−1501, 1−1601, 1−1701, 1−1801, and 1−1901. If a reaction obeys first-order kinetics, the values of the rate constants for all of the point segments are expected to be time-independent and have the same value. A factor that should be taken into account of the data in Table 5 when compared to that in Table 4 and Figures 1−3 is that the former corresponds to 2000 points over the first half-lives of the reactions and the latter to 2000 points over more than

TABLE 5. Apparent Rate Constants As a Function of Degree of Conversion and [MeO⁻][a]

15 mM k_{app}/s^{-1}	±[b]	30 mM k_{app}/s^{-1}	±[b]	60 mM k_{app}/s^{-1}	±[b]	120 mM k_{app}/s^{-1}	±[b]	segment[c]
0.294	0.011	0.855	0.032	2.941	0.199	10.420	0.200	1
0.191	0.004	0.542	0.016	1.792	0.097	7.320	0.055	2
0.178	0.001	0.452	0.012	1.330	0.048	5.510	0.052	3
0.173	0.001	0.417	0.010	0.101	0.040	4.340	0.051	4
0.170	0.002	0.395	0.009	0.977	0.033	3.600	0.044	5
0.169	0.001	0.363	0.008	0.776	0.022	3.150	0.056	6
0.172	0.001	0.357	0.009	0.713	0.019	1.630	0.060	7
0.173	0.002	0.357	0.008	0.701	0.019	1.517	0.062	8
0.175	0.001	0.357	0.009	0.696	0.019	1.473	0.065	9
0.174	0.001	0.358	0.009	0.694	0.019	1.451	0.067	10
0.174	2.000	0.359	0.009	0.694	0.019	1.439	0.069	11
0.174	0.002	0.360	0.010	0.693	0.020	1.432	0.071	12
0.174	0.002	0.360	0.010	0.693	0.020	1.427	0.072	13
0.175	0.002	0.360	0.010	0.692	0.020	1.424	0.074	14
0.175	0.002	0.361	0.010	0.692	0.021	1.421	0.076	15
0.175	0.002	0.361	0.010	0.692	0.022	1.420	0.078	16
0.175	0.002	0.362	0.011	0.694	0.022	1.419	0.080	17
0.175	0.002	0.362	0.011	0.694	0.022	1.418	0.082	18
0.175	0.002	0.363	0.012	0.694	0.022	1.418	0.084	19
0.175	0.002	0.363	0.012	0.695	0.022	1.417	0.086	20
0.174	0.002	0.364	0.012	0.695	0.022	1.417	0.080	21
0.174	0.002	0.364	0.012	0.696	0.023	1.418	0.090	22
0.174	0.002	0.365	0.013	0.696	0.023	1.417	0.092	23
0.174	0.002	0.365	0.013	0.697	0.024	1.418	0.094	24

[a]Average of three sets of 15−20 stopped-flow repetitions. Data are listed in Tables S1−S4 (Supporting Information). [b]Average deviation of a set. [c]Data segment of analysis; see text for explanation.

four half-lives. This difference means that the data segments for Table 5 begin at shorter times than those in Table 4 and Figures 1−3.

What is immediately apparent in Table 5 is that, in all four series of reactions, with [MeO⁻] ranging from 15 to 120 mM, the k_{app}−time profiles begin at relatively high values of k_{app} and decay with time to steady-state values. Although it might be argued that the standard deviations of the short time points in Figures S1−S4 (Supporting Information) are relatively high, the mean values of three determinations have a small degree of variance and are certainly significant.

It is of interest to determine how the magnitude of K_1 must be adjusted in order for calculated k_2' values to be independent of [MeO⁻] according to the mechanism in Scheme 1. The data in Table 6 show the convergence of k_2' obtained from data from [MeO⁻] equal 120 mM with that from data from the 15 mM simulation (the value of k_2 in the simulation was 17.30 M^{-1} s^{-1}). It would appear that the value of K_1 would have to be of the order of 0.10 for the k_2' values obtained at [MeO⁻] equal to 120 and 15 mM to be within experimental error of each other. The latter is clearly out of the range of the experimental values of K_1.[14,20]

TABLE 7. Simulated Values of the Ratios of Rates of Formation and Decay of Complex II

[MeO⁻]	extent of reaction (ER)	$k_2[MeO^-][TNA]_{equil}/k_{-2}[TNA]_0(ER)$[a]
120	0.1	13 557
120	0.5	1506
120	0.9	167.6
60	0.1	7726
60	0.5	858.5
60	0.9	95.4
30	0.1	4153
30	0.5	461.5
30	0.9	51.2
15	0.1	2158
15	0.5	239.8
15	0.9	26.6

[a]$[TNA]_{equil} = (1 - ER)[TNA]_0/(K_1[MeO^-] + 1)$; ER = extent of reaction.

It is possible that the neglect of the reverse rate constant k_{-2} gives rise to error in the simulations. Instantaneous rates at various values of ER and [MeO⁻] were calculated using the expression, $k_2[MeO^-][TNA]_{equil}/k_{-2}[TNA]_0(ER)$, in which the units cancel. Calculations of the relative instantaneous rates at 10, 50, and 90% conversion are shown in Table 7. The data above show that the assumption that product formation is essentially irreversible, as expected due to the large value of K_2 (equal to 17 000 M^{-1}), is valid and that the reaction goes to completion rather than to an equilibrium state.

Discussion

A very likely mechanism for the transformation of TNA to complex **II** is the reversible formation of a "reactant

SCHEME 2. Reversible Consecutive Mechanism for the Formation of Complex II during the Reaction of TNA with Methoxide Ion in Methanol

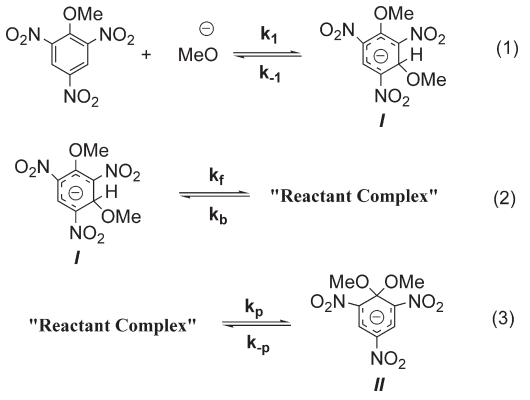

TABLE 6. Effect of the K_1 Magnitude on the Value of the Apparent Second-Order Rate Constants (k_2') Obtained from Simulated Data for the Mechanism in Scheme 1

K_1/M^{-1}	k_{app} (120 mM)/s^{-1}	k_2' (120 mM)/M^{-1} s^{-1}	k_{app} (15 mM)/s^{-1}	k_2' (15 mM)/M^{-1} s^{-1}
2.71	1.567	13.08	0.2499	16.60
2.00	1.674	13.95	0.2520	16.80
1.00	1.854	15.45	0.2557	17.05
0.50	1.959	16.33	0.2576	17.17
0.25	2.016	16.80	0.2586	17.24
0.10	2.052	17.10	0.2592	17.28
0.050	2.064	17.20	0.2594	17.29
0.025	2.070	17.25	0.2594	17.29
0.0125	2.073	17.28	0.2595	17.30

SCHEME 3. Possible Reaction of Complex I with Methoxide Ion to Form the Dianion Complex III ("Reactant Complex" = III?), Which Eliminates Methoxide Ion to Produce Complex II

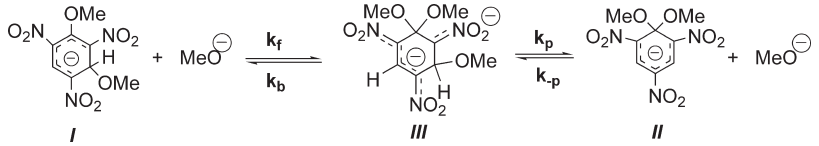

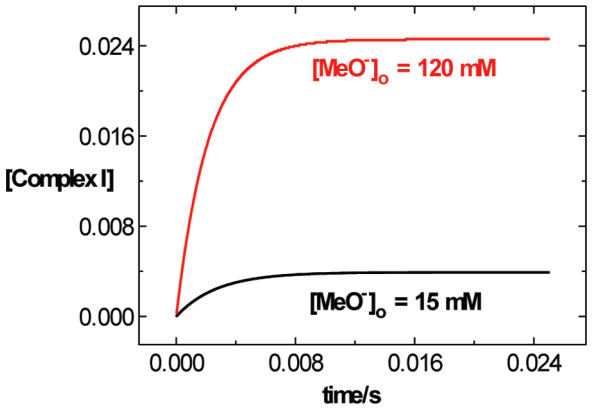

FIGURE 4. Simulated concentration−time plots for the reaction of TNA (0.1 mM) with [MeO^-] equal to 15 and 120 mM.

complex" by conversion of the σ complex (**I**), as shown in Scheme 2. We are reluctant to designate this species as the π complex because it could form directly from the reactants and then partition between the two σ complexes, **I** and **II**. That being the case, the overall result would be the same as expected for Scheme 1. A reversible consecutive mechanism that takes into account all of the experimental kinetic data is illustrated in Scheme 2. The rapidly decaying values of k_{app} at short times are characteristic for reactions in which an intermediate absorbs at the wavelength where the evolution of product is monitored, and the decreasing k_{app} at short times are due to the decay of the intermediate.

A plausible structure of the "reactant complex" is the dianion complex **III**. Servis[6] found that, in the presence of 1.0 equiv of methoxide ion, the rapid formation of complex **I** was followed by the slower transformation of complex **I** to complex **II**. However, upon addition of more than 1 equiv of methoxide ion, new ^{1}H NMR resonances appeared at 6.13 and 8.80 ppm in the ratio of 1:1. He assigned these resonances to the dianion complex **III**.[26] A possible reaction sequence for the formation of **III** is illustrated in Scheme 3. It must be pointed out that the conditions of NMR studies[6] differ considerably from those in the kinetic study, and the most pertinent differences are the methoxide concentrations (< 0.8 M in the NMR study and < 0.12 M in the our study) and the solvent (DMSO in the NMR study and methanol in our study).

It may appear possible that the "exalted" k_{app} values at short times (Tables 5 and S1−S4 (Supporting Information)) are plausibly explained by assuming that the reaction forming complex **I** has not quite reached equilibrium at short times and that the observed kinetic process is contaminated by that rapid reaction. The latter appeared to be a reasonable assumption, and we tested that possibility by simulating the time necessary for the reaction leading to complex **I** to come to equilibrium under conditions where the slower formation of complex **II** was neglected. The simulation results are illustrated in Figure 4 for the reaction of TNA (0.1 mM) with MeO^- (15 and 120 mM). The times necessary to reach the plateau regions of the two plots are indicative of the time necessary for reaction (1) (Scheme 2) to reach the equilibrium state. The plateau regions for both curves (Figure 4) are reached during the same time interval (10−15 ms). From the latter, we conclude that equilibrium is established prior to the shortest kinetic time point (15 ms) for the slowest reaction ([MeO^-] = 15 mM) and prior to the sixth time point (15 ms) for the other extreme ([MeO^-] = 120 mM). The time to reach equilibrium in reaction (1) is dependent on (k_1[MeO^-] + k_{-1}), and the values of this term are 464 ([MeO^-] = 120 mM) and 364 ([MeO^-] = 15 mM). From the latter, we conclude that the time to reach equilibrium is not an important factor in the "exalted" rate constants at short times. The plots in Figure 4 also illustrate another point that is in opposition to the latter explanation. If the kinetic process observed is contaminated by absorbance due to the formation of complex **I**, this positive absorbance would give rise to an increase in k_{app} rather than the decreasing values observed at short times. Absorbance values at short times actually decrease with time and can readily be explained by the decay of an intermediate, as proposed above.

The question as to why the 1,3-complex is formed more rapidly than the more stable 1,1-complex was addressed by Bernasconi.[19] A comparison of the known rate-retarding effect[27] due to ground-state stabilization during the hydrolysis of the *p*-methoxydiazonium ion was cited in support of the relative rates on unsubstituted versus methoxy substituted ring positions. In the latter case, the unsubstituted benzenediazonium ion was observed to react about 6000 times faster than the *p*-methoxydiazonium ion.

The reactions of 1-X-2,4,6-trinitrobenzenes (where X is alkyloxy or aryloxy groups) with nucleophiles have been classified as K3T1, K3T3, K1T1, or K1T3 by the Buncel group,[28] where, for example, K3T1 represents kinetic control (K3) by attack at the 3-position and T1 by thermodynamic control by attack at the 1-position. The classification was supported by a number of papers from that group.[29] The Buncel group[28,29] continued to assume that these reactions

(26) Xue, X. Unpublished work has computed relative Gaussian energies of TNA, complex **I**, complex **II**, and complex **III** in methanol to be equal to 0, −3.3, −6.9, and −4.0 kcal/mol, respectively.

(27) Corssley, M. L.; Kienle, R. H.; Benbrook, C. H. *J. Am. Chem. Soc.* **1940**, *62*, 14.

(28) Buncel, E.; Dust, J. M.; Manderville, R. A.; Tarkka, R. M. *Can. J. Chem.* **2003**, *81*, 443.

(29) (a) Buncel, E.; Murarka, S. K.; Norris., A. R. *Can. J. Chem.* **1984**, *62*, 534. (b) Buncel, E.; Dust, J. M.; Jonczyk, A.; Manderville, R. A.; Onyido, I. *J. Am. Chem. Soc.* **1992**, *114*, 5610. (c) Manderville, R. A.; Buncel, E. *J. Am. Chem. Soc.* **1993**, *115*, 8985. (d) Buncel, E.; Tarkka, R. M.; Dust, J. M. *Can. J. Chem.* **1994**, *72*, 1709. (e) Buncel, E.; Dust, J. M.; Terrier, F. *Chem. Rev.* **1995**, *95*, 2261.

are described by the competing mechanism described in Scheme 1.

The first reaction in Scheme 2 may consist of two steps involving a species other than the π complex, but at this stage of our investigation, we are not ready to suggest that much detail in our mechanism. Our conclusions at this time are that the formation of the 1,1-complex does not take place according to the accepted mechanism in Scheme 1 and that the 1,3-complex lies on the reaction coordinate for the formation of the thermodynamically more stable **II**. The dianion σ complex (Scheme 3) is a reasonable suggestion of the structure of the intermediate. The detailed mechanism of the formation of the σ complexes of TNA and TNB with methoxide ion and other nucleophiles is under investigation.

Experimental Section

TNA was obtained commercially and was recrystallized from methanol before use. No impurities could be detected by H^1 NMR spectrometry. Methanol was of the highest grade available and used without further purification. Sodium methoxide solutions were prepared by allowing freshly cut sodium slices to react in methanol under a nitrogen atmosphere.

Kinetic experiments were carried out using a Hi-Tech SX2 stopped-flow spectrometer installed in a glovebox and kept under a nitrogen atmosphere. The temperature was controlled at 20 °C using a constant temperature flow system connected directly to the reaction cell through a bath situated outside of the glovebox. All stopped-flow experiments included recording 15−20 absorbance−time profiles at 485 nm. Each experiment was repeated three times. The 2000 point absorbance−time curve data were collected over either 1+ or 4+ half-lives (HLs).

Absorbance−time (abs−*t*) profiles for product evolution were analyzed individually by two different procedures. The first step in both procedures was to convert the abs−*t* profiles to (1 − ER)−time profiles where ER denotes the extent of reaction. This was carried out by dividing each absorbance value by the infinity value obtained from the product extinction coefficient and the reactant concentration and subtracting the value from 1.0. This procedure gave (1 − ER)−time profiles that decayed from (1 − ER) = 1 for either one or four HLs depending on which analysis procedure was used. For pseudo-first-order kinetic analysis, the (1 − ER)−time profiles were converted to ln(1 − ER)−time profiles. For further processing, the individual four HL (1 − ER)−time profiles were first averaged to give the average profiles.

The first kinetic procedure used was simply a least-squares linear correlation of the ln(1 − ER)−time profiles to give the apparent pseudo-first-order rate constants over either one, two, three, or four HLs. These values are recorded in the Results section. The second procedure involved recording the abs−time profiles over slightly more than the first HL, followed by the sequential 24 linear correlations described in the Results section. Figures S1−S4 (Supporting Information) were included to show the difficulty of differentiating between the simple one-step mechanism and more complex mechanisms. The deviations from apparent first-order kinetics *might* be considered as negligible based upon these ln(1 − ER)−time profiles.

Acknowledgment. This work was supported by the National Science Foundation, Grant ARRA: CHE-0923654.

Supporting Information Available: Tables and figures of kinetic data under various conditions. This material is available free of charge via the Internet at http://pubs.acs.org.